Models of the Cytochromes *b*. Low-Spin Bis-Ligated (Porphinato)iron(III) Complexes with "Unusual" Molecular Structures and NMR, EPR, and Mössbauer Spectra

Martin K. Safo,[1a] Govind P. Gupta,*[,1b] C. Todd Watson,[1c] Ursula Simonis,*[,1d] F. Ann Walker,*[,1c] and W. Robert Scheidt*[,1a]

Contribution from the Department of Chemistry and Biochemistry, University of Notre Dame, Notre Dame, Indiana 46556, Department of Physics, The Pennsylvania State University, State College, Pennsylvania 16802, Department of Chemistry, University of Arizona, Tucson, Arizona 85721, and Department of Chemistry and Biochemistry, San Francisco State University, San Francisco, California 94132. *Received January 15, 1992*

Abstract: The synthesis and characterization of the following bis-pyridine and bis-imidazole complexes of (tetramesitylporphinato)iron(III) are reported: $[Fe(TMP)(4\text{-}NH_2Py)_2]ClO_4$, **1**, $[Fe(TMP)(3\text{-}EtPy)_2]ClO_4$, **2**, $[Fe(TMP)(3\text{-}ClPy)_2]ClO_4$, **3**, $[Fe(TMP)(2\text{-}MeHIm)_2]ClO_4$, **4**, $[Fe(TMP)(4\text{-}CNPy)_2]ClO_4$, **5**, and $[Fe(TMP)(3\text{-}CNPy)_2]ClO_4$, **6**. The crystal structures of complexes **2**, **3**, and **5** are reported. All three complexes have relative perpendicular alignment of the axial ligands with bond lengths consistent with low-spin iron(III). The porphinato cores are strongly S_4 ruffled; the Fe-N_p bonds show a commensurate shortening. EPR investigations reveal "large g_{max}" type EPR spectra for complexes **1**-**4**, with complexes **2**, **3**, and **4** having unusually low g values (<3.2). Complex **1** has a "normal" "large g_{max}" g value of 3.40. Complexes **5** and **6** have axial EPR spectra with $g_\perp = 2.53$ and $g_\parallel = 1.56$ or $g_\perp = 2.62$ and $g_\parallel$ unresolved, which result from a substantial change in the usual ground state of low-spin (porphinato)iron(III) complexes, $(d_{xy})^2(d_{xz},d_{yz})^3$, to that having a predominantly $(d_{xz},d_{yz})^4(d_{xy})^1$ ground state. Complexes **2**, **3**, **4**, and **5** have been characterized by Mössbauer spectroscopy. The Mössbauer isomer shifts (δ) range from 0.18 to 0.20 mm/s and the quadrupole splittings (ΔE_Q) from 0.97 to 1.48 mm/s. The quadrupole splittings, like the EPR g values of these complexes, are unusually low, compared with ΔE_Q values of $\sim$1.7-1.8 mm/s expected for imidazole complexes with perpendicular axial ligand orientation. The ^1H NMR isotropic shifts at -80 °C (193 K) of the pyrrole protons of all complexes except **1** and **2**, but including additional low-spin bis-pyridine complexes with 4-NMe_2, 3,4-Me_2, 3,5-Me_2, 4-Me, and 3-Me substituents and pyridine itself as axial ligands, varied from -39.5 ppm (4-NMe_2Py) to -6.5 ppm (4-CNPy) through this series. This result indicates a smooth change from an electronic ground state which is largely $(d_{xy})^2(d_{xz},d_{yz})^3$ to one which is at least 50% $(d_{xz},d_{yz})^4(d_{xy})^1$ in nature at 193 K for the $(4\text{-}CNPy)_2$ complex, supporting the conclusions reached on the basis of the variation of EPR and Mössbauer parameters observed at 77 K and below.

Introduction

The crystal structures of a number of heme proteins that have either one or two axial histidines bound to the iron have been reported.[2-15] In each of these structures it is found that the axial histidine plane is fixed in a particular orientation with respect to its projection on the heme plane by a combination of the covalent attachment of the imidazole ring of the histidine residue to the protein backbone, hydrogen bonding of the imidazole N-H proton to other protein residues, and the packing of other amino acid side chains in the heme pocket. It has been suggested that the particular orientation of the axial histidine plane with respect to the heme axes and, for bis-histidine-coordinated heme proteins, the relative orientation of the two histidine planes with respect to each other are important in modeling the spectroscopic and possibly also the redox properties of these heme proteins.[16-22]

Many heme proteins, including the cytochromes *b* of mitochondrial ubiquinone-cytochrome *c* oxidoreductase[23,24] and the structurally and functionally related cytochrome b_6 of chloroplasts,[23,24] exhibit the "large g_{max}" type EPR spectra[25] having only one resolved feature at $g > 3.4$ at very low temperatures. In addition, at least one of their reduction potentials at ambient temperatures ($E_{m,7}$ = 93 and -34 or 62 and -20 mV vs SHE for b_{562} and b_{566} for bovine heart[26a] or yeast[26c] mitochondria, respectively) is much higher than that of bovine microsomal cyto-

(1) (a) The University of Notre Dame. (b) The Pennsylvania State University. Current address: Department of Physics, Lucknow University, Lucknow, 226 007 India. (c) The University of Arizona. (d) San Francisco State University.

(2) Mathews, F. S.; Czerwinski, E. W.; Argos, P. In *The Porphyrins*; Dolphin, D., Ed.; Academic Press: New York, 1979; Vol. VII, pp 108-147.
(3) Timkovich, R. In *The Porphyrins*; Dolphin, D., Ed.; Academic Press: New York, 1979; Vol. VII, pp 241-294.
(4) Mathews, F. S.; Bethge, P. H.; Czerwinski, E. W. *J. Biol. Chem.* **1979**, *254*, 1699-1706. Lederer, F.; Glatigny, A.; Bethge, P. H.; Bellamy, H. D.; Mathews, F. S. *J. Mol. Biol.* **1981**, *148*, 427-448.
(5) Takano, T. *J. Mol. Biol.* **1977**, *110*, 537-568, 569-584. Phillips, S. E. V. *J. Mol. Biol.* **1980**, *142*, 531-554.
(6) Perutz, M. F.; Fermi, G.; Luisi, B.; Shaanan, B.; Liddington, R. C. *Acc. Chem. Res.* **1987**, *20*, 309-321.
(7) Pierrot, M.; Haser, R.; Frey, M.; Payan, F.; Astier, J.-P. *J. Biol. Chem.* **1982**, *257*, 14341-14348.
(8) Higuchi, Y.; Kusunoki, M.; Matsuura, Y.; Yasuoka, N.; Kakudo, M. *J. Mol. Biol.* **1984**, *172*, 109-139.
(9) Matsuura, Y.; Takano, T.; Dickerson, R. E. *J. Mol. Biol.* **1982**, *156*, 389-409.
(10) Bell, J. A.; Korszun, Z. R.; Moffat, K. *J. Mol. Biol.* **1981**, *147*, 325-335.
(11) Takano, T.; Dickerson, R. E. *J. Mol. Biol.* **1981**, *153*, 79-94.
(12) Kuriyan, J.; Wilz, S.; Karplus, M.; Petsko, G. A. *J. Mol. Biol.* **1986**, *192*, 133-154.
(13) Finzel, B. C.; Weber, P. C.; Hardman, K. D.; Salemme, F. R. *J. Mol. Biol.* **1985**, *186*, 627-643.
(14) Carter, D. C.; Melis, K. A.; O'Donnell, S. E.; Burgess, B. K.; Furey, W. F.; Wang, B.-C.; Stout, C. D. *J. Mol. Biol.* **1985**, *184*, 279-295.
(15) Finzel, B. C.; Poulos, T. L.; Kraut, J. *J. Biol. Chem.* **1984**, *259*, 13027-13036.
(16) Korsun, Z. R.; Moffat, F.; Frank, K.; Cusanovich, M. A. *Biochemistry* **1982**, *21*, 2253-2258.
(17) Scheidt, W. R.; Chipman, D. M. *J. Am. Chem. Soc.* **1986**, *108*, 1163-1167.
(18) Walker, F. A. *J. Am. Chem. Soc.* **1980**, *102*, 3254-3256.
(19) Walker, F. A.; Benson, M. *J. Phys. Chem.* **1982**, *88*, 3495-3499.
(20) Walker, F. A.; Buehler, J.; West, J. T.; Hinds, J. L. *J. Am. Chem. Soc.* **1983**, *105*, 6923-6929.
(21) Zhang, H.; Simonis, U.; Walker, F. A. *J. Am. Chem. Soc.* **1990**, *112*, 6124-6126.
(22) Satterlee, J. D. In *Metal Ions in Biological Systems*; Sigel, H., Eds.; Marcel Dekker: New York, 1987; Vol. 21, pp 121-185.
(23) Widger, W. R.; Cramer, W. A.; Herrmann, R. G.; Trebst, A. *Proc. Natl. Acad. Sci. U.S.A.* **1984**, *81*, 674-678.
(24) Daldar, F.; Tokito, M. K.; Davidson, E.; Faham, M. *EMBO J.* **1989**, *13*, 3951-3961.
(25) (a) Orme-Johnson, N. R.; Hansen, R. E.; Beinert, H. *Biochem. Biophys. Res. Commun.* **1971**, *45*, 871-878. (b) Salerno, J. C. *J. Biol. Chem.* **1984**, *259*, 2331-2336. (c) Salerno, J. C. *FEBS Lett.* **1983**, *162*, 257-261. (d) Leigh, J. S.; Ericinska, M. *Biochim. Biophys. Acta* **1975**, *387*, 95-106. (e) Ericinska, M.; Oshino, R.; Oshino, N.; Chance, B. *Arch. Biochem. Biophys.* **1973**, *157*, 431-445. (f) Bergström, J. *FEBS Lett.* **1985**, *183*, 87-90.
(26) (a) Nelson, B. D.; Gellerfors, P. *Biochim. Biophys. Acta* **1974**, *357*, 358-364. (b) Von Jagow, G.; Schagger, H.; Engel, W. D.; Hachenberg, H.; Kolb, H. J. C. In *Energy Conservation in Biological Membranes*; Schafer, G., Klingenberg, M., Eds.; Springer: Berlin, 1978; pp 43-52. (c) T'sai, A.-H.; Palmer, G. *Biochim. Biophys. Acta* **1983**, *722*, 349-363.

0002-7863/92/1514-7066$03.00/0

chrome b_5, whose epr spectrum is of the normal rhombic "B hemichrome" type ($g_1 = 3.03$, $g_2 = 2.23$, $g_3 = 1.43$)[27] and reduction potential is near 0 mV vs SHE.[28] To understand the origin of the "large g_{max}" type of EPR spectrum we have previously performed a combined X-ray crystallographic, EPR, and Mössbauer spectroscopic investigation of frozen solutions and single crystals of two model hemes.[29] From these studies we were able to show that the "large g_{max}" type of EPR spectrum is observed when planar axial ligands are perpendicularly aligned, whereas a normal rhombic EPR spectrum is observed when the two ligands are in parallel planes.[29]

The effects of relative parallel or perpendicular axial ligand orientation are manifested not only in the EPR g values but also in the NMR spectra of both model hemes and heme proteins. LaMar and co-workers have shown[22,30-33] that the orientation of the axial histidine plane(s) in heme proteins controls the anisotropy of spin delocalization to the periphery of the heme group and nearby side chain substituents. The reason that a planar axial ligand, or more generally an axial ligand with a π-symmetry lone pair of electrons, can affect the magnetic anisotropy of the heme is that the *typical* d-electron configuration $(d_{xy})^2(d_{xz},d_{yz})^3$ of low-spin Fe(III) hemes has a single unpaired electron in the formally degenerate d_π orbitals, which can overlap with the filled $3e(\pi)$ orbitals of the porphyrin ring[34] to allow spin delocalization to the periphery of the heme ring through porphyrin $\rightarrow$ Fe(III) π donation.[35,36] Both the iron d_π and porphyrin $3e(\pi)$ orbitals are degenerate pairs in the absence of substituent or axial ligand effects.[18,34,36] However, the presence of a π-symmetry orbital on one axial ligand (or two, unless they are oriented perpendicular to each other) can remove this degeneracy by aligning the half-filled d_π orbital such that it can interact with the π-symmetry lone pair orbital to allow L $\rightarrow$ M π donation from axial ligand to Fe(III) ion.[19] This serves to produce large isotropic shifts at the β-pyrrole positions of rings I and III of the heme if the axial ligand planes lie over N_{II} and N_{IV}, or pyrrole rings II and IV if they lie over N_I and N_{III}, probably due to a combination of the contact interaction and the in-plane dipolar interaction, both of which are significant for low-spin Fe(III) porphyrins.[19,37]

For so-called "hindered" model hemes, such as (tetraphenylporphinato)iron(III) complexes having substituents at both ortho positions of the four phenyl rings, we have recently shown that NMR spectroscopy can be used as a sensitive tool to determine the relative orientation of the axial ligands.[38] From 1-D and 2-D NMR investigations we found that axial ligands, such as 2-methylimidazole (2-MeHIm), are hindered in rotation about the Fe–L bond at low temperatures.[38] In order to explain the observed resonance and coupling pattern we concluded that at low temperatures the axial ligands are fixed in perpendicular orientations over the meso positions.[38] This conclusion is nicely supported by a combination of EPR and Mössbauer spectroscopic and X-ray crystallographic studies of the related complex, $[Fe(TMP)L_2]ClO_4$ (TMP = tetramesitylporphyrin; L = 4-(dimethylamino)pyridine, 4-NMe_2Py).[39] This study revealed that the pyridine ligands lie over the meso positions in perpendicular planes.[40,41] This is in contrast to the corresponding Fe^{III}(OEP) (and presumably Fe^{III}(TPP), based on EPR spectral type[42]) complex, which prefers to place its axial ligands in parallel planes lying over the meso positions in the solid state and in frozen solution.[40,41] In fluid solution, however, NMR studies confirmed that nonhindered axial ligands, such as *N*-methylimidazole (NMeIm),[39] bound to either Fe(TPP) or Fe(TMP) are able to rotate freely, even at −90 °C in CD_2Cl_2.[43] One resonance is observed for the eight pyrrole protons, and hence the degeneracy of the porphyrin orbitals is not lifted.

Careful analysis of the structure of $[Fe(TMP)(4\text{-}NMe_2Py)_2]ClO_4$[40,41] indicates that the binding of the two 4-(dimethylamino)pyridine ligands causes the nonbonded interactions between the *o*-methyl groups of TMP and the pyridine ligands to produce a strongly ruffled porphyrin core having two oblong "cavities" at right angles to each other, one above and one below the plane of the porphyrin ring, which hold the axial ligands in perpendicular planes over the meso positions. Consistent with the structure of $[Fe(TMP)(4\text{-}NMe_2Py)_2]^+$,[41] the EPR and Mössbauer spectra are similar to those previously observed for $[Fe(TPP)(2\text{-}MeHIm)_2]^+$,[29,44] in which the axial ligands are also in perpendicular planes lying over the meso positions. Hence both solid-state and solution measurements show that we can produce a series of interesting model complexes in which the 2- and 6-phenyl substituents influence the relative and absolute orientation of axial ligand planes in solution at low temperatures,[38] as well as in the solid state.[40,41]

In an attempt to obtain further information about the importance of the 2,6-phenyl substituents on axial ligand orientation and spectroscopic properties of low-spin iron(III) tetraphenylporphyrins, we have investigated the structures and spectroscopic properties of a series of additional bis-pyridine complexes of Fe^{III}(TMP), in which the σ-basicity of the pyridine ligand was varied from the highly basic 4-NMe_2Py ($pK_a(BH^+) = 9.70$[44]) to the very weakly basic 3-CNPy ($pK_a(BH^+) = 1.45$[45]) and 4-CNPy (estimated $pK_a(BH^+) = 1.1$[46]). We have found that while the structures of the $[Fe(TMP)L_2]^+$ complexes are quite similar, the NMR, EPR, and Mössbauer spectra of the series of complexes vary in a smooth manner which is indicative of a change in the electronic ground state of low-spin Fe(III) from predominantly

(27) (a) Bois-Poltoratsky, R.; Eherenberg, A. *Eur. J. Biochem.* **1967**, *2*, 361–365. (b) Passon, P. G.; Reed, D. W.; Hultquist, D. E. *Biochim. Biophys. Acta* **1972**, *275*, 51–61.

(28) (a) Walker, F. A.; Emrick, D.; Rivera, J. E.; Hanquet, B. J.; Buttlaire, D. H. *J. Am. Chem. Soc.* **1988**, *110*, 6234–6240. (b) Reid, L. S.; Taniguchi, V. T.; Gray, H. B.; Mauk, A. G. *J. Am. Chem. Soc.* **1982**, *104*, 7516.

(29) Walker, F. A.; Huynh, B. H.; Scheidt, W. R.; Osvath, S. R. *J. Am. Chem. Soc.* **1986**, *108*, 5288–5297.

(30) La Mar, G. N.; Burns, P. D.; Jackson, J. T.; Smith, K. M.; Langry, K. C.; Strittmatter, P. *J. Biol. Chem.* **1981**, *256*, 6075–6079.

(31) McLachlan, S. J.; La Mar, G. N.; Lee, K. B. *Biochim. Biophys. Acta* **1988**, *957*, 430–445.

(32) Unger, S. W.; Jue, T.; La Mar, G. N. *J. Magn. Reson.* **1985**, *61*, 448–456.

(33) (a) Thanabal, V.; de Ropp, J. S.; La Mar, G. N. *J. Am. Chem. Soc.* **1987**, *109*, 265–272. (b) Emerson, S. D.; La Mar, G. N. *Biochemistry* **1990**, *29*, 1545–1556, 1556–1566.

(34) Longuet-Higgins, H. C.; Rector, C. W.; Platt, J. R. *J. Chem. Phys.* **1950**, *18*, 1174–1181.

(35) La Mar, G. N.; Walker, F. A. *J. Am. Chem. Soc.* **1973**, *95*, 1782–1790.

(36) La Mar, G. N.; Walker, F. A. In *The Porphyrins*; Dolphin, D., Ed.; Academic Press: New York, 1979; Vol. IV, pp 61–157.

(37) (a) Horrocks, W. D.; Greenberg, E. S. *Biochim. Biophys. Acta* **1973**, *322*, 38–44. (b) Horrocks, W. D.; Greenberg, E. S. *Mol. Phys.* **1974**, *27*, 993–999.

(38) Walker, F. A.; Simonis, U. *J. Am. Chem. Soc.* **1991**, *113*, 8652–8657.

(39) Abbreviations used include the following: 1-MeIm, 1-methylimidazole; 2-MeHIm, 2-methylimidazole; 1-VinIm, 1-vinylimidazole; HIm, imidazole; 2-MeHBzim, 2-methylbenzimidazole; Py, pyridine; 4-NMe_2Py, 4-(dimethylamino)pyridine; 3- or 4-MePy, 3- or 4-methylpyridine (3- or 4-picoline); 4-NH_2Py, aminopyridine; 3-EtPy, 3-ethylpyridine; 3- or 4-CNPy, 3- or 4-cyanopyridine; 3-ClPy, 3-chloropyridine; 3,5- or 3,4-Me_2Py, 3,5- or 3,4-lutidine; OEP, dianion of octaethylporphyrin; TPP, dianion of *meso*-tetraphenylporphyrin; TMP, dianion of *meso*-tetramesitylporphyrin; 2,6-Cl_2PP, dianion of *meso*-tetra(2,6-dichlorophenyl)porphyrin; Proto IX, dianion of protoporphyrin IX; OEC, dianion of octaethylchlorin; OEiBC, dianion of octaethylisobacteriochlorin.

(40) Safo, M. K. Ph.D. Thesis, University of Notre Dame, 1991.

(41) Safo, M. K.; Gupta, G. P.; Walker, F. A.; Scheidt, W. R. *J. Am. Chem. Soc.* **1991**, *113*, 5497–5510.

(42) Walker, F. A.; Reis, D.; Balke, V. L. *J. Am. Chem. Soc.* **1984**, *106*, 6888–6898.

(43) Walker, F. A.; Simonis, U.; Zhang, H.; Walker, J. M.; Ruscitti, T. M.; Kipp, C.; Amputch, M. A.; Castillo, B. V.; Cody, S. H.; Wilson, D. L.; Graul, R. E.; Yong, G. J.; Tobin, K.; West, J. T.; Barichievich, B. A. *New J. Chem.*, in press.

(44) Albert, A. In *Physical Methods in Heterocyclic Chemistry*; Katritzky, A. R., Ed.; Academic Press: New York, 1971; Vol. III, pp 1–26.

(45) Albert, A. In *Physical Methods in Heterocyclic Chemistry*; Katritzky, A. R., Ed.; Academic Press: New York, 1971; Vol. I, pp 1–108.

(46) The reported pK_a of the conjugate acid of 4-cyanopyridine is 1.90.[45] However, on the basis of the dependence of the pK_as of the conjugate acids of fourteen other pyridines (3-NO_2, 3-CN, 3-Cl, 3-F, 4-Cl, 3-OCH_3, H, 3-Me, 4-Me, 3,5-Me_2, 3,4-Me_2, 4-OMe, 4-NH_2, and 4-NMe_2) on the Hammett σ constants for the substituents,[47] we estimate that the pK_a of 4-CNPyH$^+$ should be 1.1 or less. We have therefore used the value 1.1 in the plots shown in Figures 5–7 and in Tables II and III.

(47) Hansch, C.; Leo, A.; Taft, R. W. *Chem. Rev.* **1991**, *91*, 165–195.

Table I. Crystal Data and Intensity Collection Parameters

	$[Fe(TMP)(3\text{-}EtPy)_2]ClO_4{\cdot}2CH_2Cl_2$	$[Fe(TMP)(4\text{-}CNPy)_2]ClO_4{\cdot}2CH_2Cl_2$	$[Fe(TMP)(3\text{-}ClPy)_2]ClO_4$
formula	$FeCl_5O_4N_6C_{72}H_{74}$	$FeCl_5O_4N_8C_{70}H_{64}$	$FeCl_3O_4N_6C_{66}H_{60}$
fw, amu	1272.5	1314.4	1163.45
space group	$P2_1/n$	$P2_1/n$	$P2_1/n$
T, K	118.0	118.0	294.5
a, Å	15.119 (4)	15.423 (8)	18.251 (3)
b, Å	21.845 (5)	21.152 (17)	18.854 (2)
c, Å	20.389 (4)	19.960 (8)	19.504 (3)
β, deg	100.90 (2)	100.56 (4)	108.93 (1)
V, Å^3	6612.4	6401.3	6348.2
Z	4	4	4
scan technique	θ–2θ	θ–2θ	θ–2θ
diffractometer	CAD4	CAD4	CAD4
cryst dimens, mm	0.5 × 0.2 × 0.7	0.2 × 0.3 × 0.4	0.4 × 0.4 × 0.7
2θ limits	4.0–50.7	4.0–52.86	4.0–156.0
radiation	Mo Kα	Mo Kα	Cu Kα
criterion for obs	$F_o > 3.0\sigma(F_o)$	$F_o > 3.0\sigma(F_o)$	$F_o > 2.5\sigma(F_o)$
no. of obsd data	7180	7197	4731
D(obsd), g/cm^3	1.27	1.36	1.22
D(calcd), g/cm^3	128	1.36	1.22
R_1	0.058	0.081	0.103
R_2	0.056	0.092	0.122

$(d_{xy})^2(d_{xz},d_{yz})^3$ to predominantly $(d_{xz},d_{yz})^4(d_{xy})^1$ as the σ-basicity of the pyridine decreases, as will be discussed below. Such a change in electronic ground state has previously been suggested for the low-spin Fe(III) complexes of chlorins.[48-50]

Experimental Section

General Information. Solvents used for synthesis of complexes **1–6** were distilled under argon prior to use. Tetrahydrofuran (THF) and benzene were distilled from sodium benzophenone ketyl. Dichloromethane, chloroform, chlorobenzene, and hexane were distilled from calcium hydride. 4-Cyanopyridine was recrystallized from dichloromethane. Other pyridines and 2-methylimidazole were obtained from Aldrich and used without further purification. Deuterated dichloromethane (Cambridge Isotopes) was dried and stored over molecular sieves (Linde 4Å). Tetramesitylporphyrin was synthesized by slight modification[41] of the procedure published by Lindsey et al.[51] [Fe(TMP)$OClO_3$] was prepared as described previously.[41] Mössbauer measurements, performed on samples obtained from crushed single crystals as wax suspensions (mp 78 °C), were made at 4.2 and/or 77 K as described previously.[52] EPR spectra were obtained at 77 and/or <30 K with a Varian E-12 EPR spectrometer operating at X-band and equipped with Varian flowing nitrogen and Air Products helium variable temperature controllers, respectively. UV–visible spectra were recorded on a Perkin-Elmer Lambda 4C spectrophotometer, and IR spectra were recorded on a Perkin-Elmer 883 spectrophotometer as KBr pellets. Proton NMR spectra were recorded on a General Electric GN-300WB spectrometer operating at 300.100 MHz, as described previously.[38] Chemical shifts were referenced to residual $CHDCl_2$ (5.32 ppm). NOESY spectra were collected on the same instrument as described previously.[38]

Synthesis of $[Fe(TMP)(3\text{-}EtPy)_2]ClO_4$, 2, [Fe(TMP)$OClO_3$] (80 mg, 0.085 mmol) and 3-EtPy[39] (92 mg, 0.853 mmol) were dissolved in about 15 mL of CH_2Cl_2. The reaction mixture was stirred briefly and the solution was filtered and then layered with hexane. X-ray quality crystals formed after 3 days.

Synthesis of $[Fe(TMP)(4\text{-}NH_2Py)_2]ClO_4$, 1, [Fe(TMP)$OClO_3$] (15 mg, 0.016 mmol) and 4-NH_2Py[39] (7.5 mg, 0.080 mmol) were dissolved in about 3 mL of CH_2Cl_2. Reaction and crystallization procedures were carried out as above, but only microcrystalline material was obtained.

Synthesis of $[Fe(TMP)(3\text{-}ClPy)_2]ClO_4$, 3, [Fe(TMP)$OClO_3$] (80 mg, 0.085 mmol) and 3-ClPy[39] (97 mg, 0.854 mmol) were dissolved in about 15 mL of CH_2Cl_2. Reaction and crystallization procedures were carried out as above. X-ray quality crystals formed after 4 days.

Synthesis of $[Fe(TMP)(2\text{-}MeHIm)_2]ClO_4$, 4. [Fe(TMP)$OClO_3$] (80 mg, 0.085 mmol) and 2-MeHIm[39] (70 mg, 0.853 mmol) were dissolved in about 15 mL of CH_2Cl_2. Reaction and crystallization procedures were carried out as above. Microcrystalline material was obtained, which was unsuitable for single-crystal X-ray structure determination.

Synthesis of $[Fe(TMP)(4\text{-}CNPy)_2]ClO_4$, 5, [Fe(TMP)$OClO_3$] (50 mg, 0.053 mmol) and 4-CNPy[39] (110 mg, 1.06 mmol) were dissolved in about 10 mL of CH_2Cl_2. Reaction and crystallization procedures were carried out as above. X-ray quality crystals formed after 4 days.

Synthesis of $[Fe(TMP)(3\text{-}CNPy)_2]ClO_4$, 6, [Fe(TMP)$OClO_3$] (60 mg, 0.064 mmol) and 3-CNPy[39] (100 mg, 0.961 mmol) were dissolved in about 10 mL of CH_2Cl_2. Reaction and crystallization procedures were carried out as above. Crystalline material was obtained after 2 days.

Structure Determinations. Crystals of $[Fe(TMP)(4\text{-}CNPy)_2]ClO_4$, **5**, $[Fe(TMP)(3\text{-}EtPy)_2]ClO_4$, **2**, and $[Fe(TMP)(3\text{-}ClPy)_2]ClO_4$, **3**, were mounted on a glass fiber and subjected to a detailed photographic examination followed by intensity data collection on an Enraf-Nonius CAD4 diffractometer. The crystals of **5** and **2** were unstable outside the mother liquor and had to be examined at low temperature (118 ± 2 K). This was done with a locally modified Syntex LT-1 low-temperature attachment. Preliminary examination of all three crystals established a four-molecule unit cell, space group $P2_1/n$. Final cell constants and complete details of the intensity collection and least-squares refinement parameters for the three complexes are summarized in Tables I and SIV. Precise cell constants were determined from least-squares refinement of 25 automatically entered reflections. Four standard reflections were monitored during each data collection for crystal movements and possible deterioration of the crystals. No significant decay was observed for two complexes, but $[Fe(TMP)(3\text{-}ClPy)_2]ClO_4$, **3**, showed a gradual but significant decrease in reflection intensities. Intensity data were reduced using the data reduction program suite of Blessing.[53] The data were corrected for background and Lorentz polarization during the data reduction. All data with $F_o \geq 3.0\sigma(F_o)$ were retained as observed for **2** and **5** and used in all subsequent refinements. For **3**, data with $F_o \geq 2.5$ were retained as observed. The structures were solved by use of MULTAN and difference Fourier maps. The full-matrix least-squares programs ALLS or ORFLS[54] were used for structure refinement. After several cycles of least-squares refinement, more than 90% of the possible hydrogen atoms were located in all three complexes. The hydrogen atom positions were idealized and included in subsequent cycles of least-squares refinement as fixed contributors (C–H = 0.95 Å and B(H) = 1.3B(C)), with additional reidealization as required. Anisotropic thermal parameters were used for all heavy atoms except for some disordered atoms of the perchlorate anion of **3**.

X-ray Structures of $[Fe(TMP)(3\text{-}EtPy)_2]ClO_4$, 2, and $[Fe(TMP)(4\text{-}CNPy)_2]ClO_4$, 5. Graphite-monochromated Mo Kα radiation (λ =

(48) Taylor, C. P. S. *Biochim. Biophys. Acta* **1977**, *491*, 137.
(49) Muhoberac, B. B.; Wharton, D. C. *J. Biol. Chem.* **1983**, *258*, 3019–3027.
(50) Muhoberac, B. B. *Arch. Biochem. Biophys.* **1984**, *233*, 682–697.
(51) Wagner, R. W.; Lawrence, D. S.; Lindsey, J. S. *Tetrahedron Lett.* **1987**, *28*, 3069–70. Lindsey, J. S.; Wagner, R. W. *Org. Chem.* **1988**, *54*, 828–836.
(52) Scheidt, W. R.; Osvath, S. R.; Lee, Y. J.; Reed, C. A.; Schaevitz, B.; Gupta, G. P. *Inorg. Chem.* **1989**, *28*, 1591–1595.
(53) Blessing, R. H. *Cryst. Rev.* **1987**, *1*, 3–58.
(54) Programs used in this study included local modifications of Main, Hull, Lessinger, Germain, Declerq, and Woolfson's MULTAN, Jacobson's ALLS, Zalkin's FORDAP, Busing and Levy's ORFFE, and Johnson's ORTEP2. Atomic form factors were from: Cromer, D. T.; Mann, J. B. *Acta Crystallogr., Sect. A* **1968**, *A24*, 321–323. Real and imaginary corrections for anomalous dispersion in the form factor of the iron atom were from: Cromer, D. T.; Liberman, D. J. *Chem. Phys.* **1970**, *53*, 1891–1898. Scattering factors for hydrogen were from: Stewart, R. F.; Davidson, E. R.; Simpson, W. T. *Chem. Phys.* **1965**, *42*, 3175–3187.

Table II. Axial Ligand Basicities, Mössbauer Parameters, and EPR g Values for Low-Spin Six-Coordinate Iron(III) Porphyrinates, $[Fe(Por)L_2]^+$, with Perpendicular Axial Ligand Orientations

complex	ligand $pK_a(BH^+)$[a]	δ[b] mm/s	ΔE_q[b] mm/s	g[b]	EPR type	ref
$[Fe(TMP)(4\text{-}NMe_2Py)_2]ClO_4$	9.70	0.20	1.74 (c)	3.48 (c)	g_{max}	41
$[Fe(TMP)(4\text{-}NH_2Py)_2]ClO_4$[c] (**1**)	9.17			3.40 (c)	g_{max}	this work
$[Fe(TMP)(2\text{-}MeHIm)_2]ClO_4$[c] (**4**)	7.56	0.20	1.48 (c)	3.17 (c)	g_{max}	this work
$[Fe(TMP)(3\text{-}EtPy)_2]ClO_4$ (**2**)	5.56	0.18	1.25 (c)	2.89 (c)	g_{max}	this work
$[Fe(TMP)(3\text{-}ClPy)_2]ClO_4$ (**3**)	2.84	0.20	1.36 (c)	3.07 (c)	g_{max}	this work
$[Fe(TMP)(3\text{-}CNPy)_2]ClO_4$ (**6**)	1.45			2.64 (c)	axial	this work
$[Fe(TMP)(4\text{-}CNPy)_2]ClO_4$ (**5**)	1.1[d]	0.20	0.97 (c)	2.53 (c)	axial	this work
$[Fe(TPP)(2\text{-}MeHIm)_2]^+$[c]	7.56[f]	0.22	1.77 (c)	3.56 (c)	g_{max}	29
				3.40 (s)	g_{max}	42
$[Fe(Proto\ IX)(2\text{-}MeHIm)_2]^+$[c]	7.56[f]	0.16	1.87 (s)	3.48[h]		36
$[Fe(TPP)(Py)_2]^+$[c,e,g]	5.22	0.16	1.25 (c)	3.70 (c)	g_{max}	57, 59
				3.4 (s)		42
$[Fe(Proto\ IX)(Py)_2]^+$[c,e]	5.22	0.28	1.95 (s)	3.53 or	g_{max}	55
		0.23	1.88 (c)	3.64[i] (s)		59

[a] pK_a values obtained from refs 44 and 45. [b] The letters in parentheses indicate measurement in the solid state (c) and a measurement in solution (s). [c] The EPR and Mössbauer parameters and structure of related complexes suggest that these complexes will have perpendicular axial ligand orientation. [d] See ref 46. [e] Two independent measurements. [f] Corrected for the presence of $2H^+$ (0.3). [g] Mössbauer quadrupole splittings and EPR g values determined independently from different sample preparations. [h] 1,2-Me_2Im used for g-value determination. [i] $g = 3.64$ obtained from Mössbauer spectral fits.

0.71073 Å) was used for all measurements at 118 K. Each structure consists of a full independent molecule in the asymmetric unit.

X-ray Structure of $[Fe(TMP)(3\text{-}ClPy)_2]ClO_4$, 3, Graphite-monochromated Cu Kα radiation (λ = 1.54184 Å) was used for all measurements at 294 K. Data were collected in shells, and at $\sin\theta/\lambda$ = 0.626, the standard intensities had dropped to ≈45% of the starting values. A crystal decay correction was applied during data reduction. The intensity data were corrected for absorption (μ = 34.8 mm^{-1}). The structure consists of a full independent molecule in the asymmetric unit. The perchlorate anion was disordered (two positions). Rigid group refinement was used for two perchlorate anions with occupancy ratios of 0.6:0.4.

Final atomic coordinates for complexes **2**, **3**, and **5** are listed in the supplemenary material (Tables SII, SIII, and SIV). Final anisotropic temperature factors, hydrogen atom positions, fixed coordinates for the perchlorate anion, and structure factor tables are also listed in the supplementary material (Tables SV–SXX).

Results

Complexes **1–6** have been characterized by ^1H NMR, EPR, and Mössbauer spectroscopy. In addition, the crystal and molecular structure of $[Fe(TMP)(3\text{-}EtPy)_2]ClO_4$, **2**, $[Fe(TMP)(3\text{-}ClPy)_2]ClO_4$, **3**, and $[Fe(TMP)(4\text{-}CNPy)_2]ClO_4$, **5**, were determined. Preliminary results of the structure of a fourth complex, $[Fe(TMP)(3\text{-}CNPy)_2]ClO_4$, **6**, were also obtained.

The EPR spectra of $[Fe(TMP)(4\text{-}NH_2Py)_2ClO_4$, **1**, $[Fe(TMP)(3\text{-}EtPy)_2]ClO_4$, **2**, $[Fe(TMP)(3\text{-}ClPy)_2]ClO_4$, **3**, and $[Fe(TMP)(2\text{-}MeHIm)_2]ClO_4$, **4**, recorded at <30 K, are unusual; they have only one discernible feature, which is similar in shape to the so-called "large g_{max}" EPR signal.[29,42] However, the single g values of **2**, **3**, and **4** are unusually low, far smaller than the g > 3.4 usually observed for such systems. The EPR g value for **2** is 2.89, while that for **3** is 3.07 and that for **4** is 3.17. $[Fe(TMP)(4\text{-}NH_2Py)_2]ClO_4$, **1**, however, has a more "normal" "large g_{max}" value of 3.40. These signals are not observed at 77 K and above. The EPR spectra of $[Fe(TMP)(4\text{-}CNPy)_2]ClO_4$, **5**, and $[Fe(TMP)(3\text{-}CNPy)_2]ClO_4$, **6**, which are observed even at 77 K, are also unusual. Complex **5** exhibits an axial EPR spectrum with $g_\perp$ = 2.53 and $g_\parallel$ = 1.56. The spectrum is illustrated in Figure 1; **6** also exhibits an axial EPR spectrum with $g_\perp$ = 2.62; unfortunately, in this case the spectrum is broadened and $g_\parallel$ is not observed. Complete g values are given in Table II together with the g values of other low-spin iron(III) complexes for comparison.[29,42,55–57]

The Mössbauer spectra of complexes **2–5** have been measured at 77 K (zero field) and are shown in Figure 2. The isomer shifts and quadrupole splittings are listed in Table II. Although the isomer shifts are similar to values reported for other low-spin (porphinato)iron(III) complexes,[56] the quadrupole splittings of the complexes are unusually small. Isomer shifts and quadrupole splittings of other representative low-spin iron(III) porphyrinates[55,58–60] are also given in Table II. The Mössbauer spectra

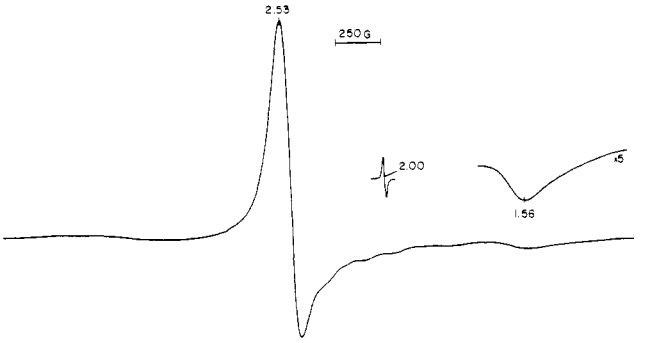

Figure 1. EPR spectrum of $[Fe(TMP)(4\text{-}CNPy)_2]ClO_4$ recorded at 77 K. The signal from DPPH (g = 2.0036) is superimposed.

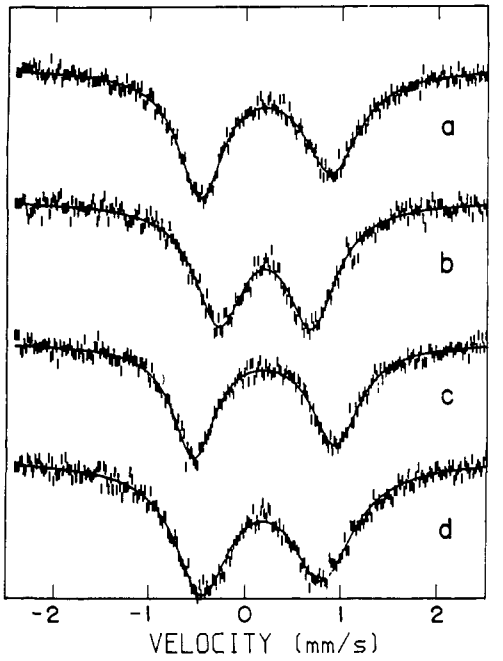

Figure 2. Mössbauer spectra of $[Fe(TMP)(3\text{-}ClPy)_2]ClO_4$ (a), $[Fe(TMP)(4\text{-}CNPy)_2]ClO_4$ (b), $[Fe(TMP)(2\text{-}MeHIm)_2]ClO_4$ (c), and $[Fe(TMP)(3\text{-}EtPy)_2]ClO_4$ (d) recorded at 77 K in zero field.

(55) Rhynard, D.; Lang, G.; Spartalian *J. Chem. Phys.* **1979**, *7*, 3715.
(56) See Table VI of ref 41.
(57) Inniss, D.; Soltis, S. M.; Strouse, C. E. *J. Am. Chem. Soc.* **1988**, *110*, 5644–5650.

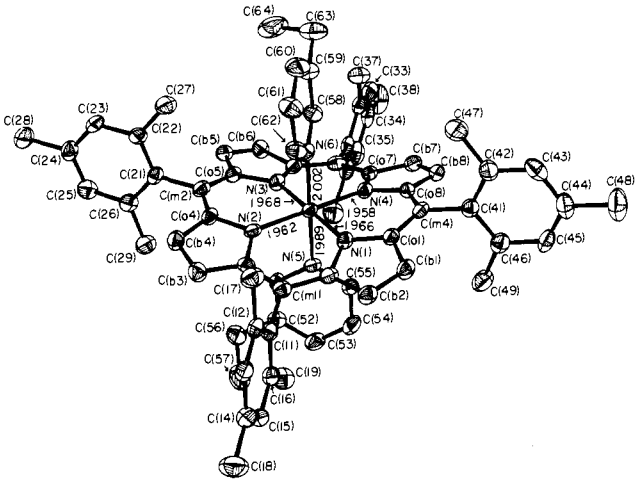

Figure 3. ORTEP diagram of $[Fe(TMP)(3\text{-}EtPy)_2]ClO_4$, **2**. Labels assigned to the crystallographically unique atoms are displayed. Atoms are contoured at the 50% probability level.

of all the complexes shown in Figure 2 exhibit significant broadening and even more broadening at 4.2 K in zero applied field; thus the Mössbauer parameters could not be determined in zero field at that temperature. Even in a strong applied field (60 kG) the spectra were broad and the hyperfine structure unresolved.

The proton NMR spectra of nine complexes, where the pyridine ligands carry substituents of varying electron donating and withdrawing character in the 3- and/or 4-positions of the pyridine ring, were measured at −80 °C in CD_2Cl_2. (Unfortunately, the 4-NH_2Py complex was not sufficiently soluble in CD_2Cl_2 at this temperature to allow its NMR spectrum to be obtained.) Assignments of proton resonances were made based on peak intensities and, among TMP resonances, on cross correlations observed in the NOESY (nuclear Overhauser and exchange spectroscopy) spectra between the *m*-H resonances and *o*- and *p*-CH_3 resonances of the mesityl rings of representative complexes (not shown). The chemical shifts of the protons of the TMP ligand for the nine $[Fe(TMP)(L)_2]^+$ complexes are listed in Table III.

The molecular structure of **2**, a representative example, is shown in Figure 3. The atom labeling schemes for the crystallographically unique atoms and bond distances in the coordination group are also displayed. As can be seen in Figures 3 and 4, the complex has axial pyridine planes with approximately perpendicular orientations. The same is true for **3** and **5**. The dihedral angles, ϕ, between the ligand plane and the closest Fe–N_p vector are 44° and 44° in **2**, 29° and 42° in **3**, and 43° and 44° in **5**. The resulting dihedral angle between the two pyridine planes is 77° in **3** and 90° in **2** and **5**. The pyridine ligand planes are nearly perpendicular to the porphyrin core, with dihedral angles of 82.9° and 86.0° in **2**, 82.8° and 75.8° in **5**, and 88.1° and 84.0° in **3**. Finally, the preliminary structure determination of $[Fe(TMP)(3\text{-}CNPy)_2]ClO_4$, **6**, shows quite similar features including an approximately perpendicular orientation for the pyridine ligands.

Averaged values for the chemically equivalent bond distances and angles in the cores of **2**, **3**, and **5** are shown in Figure 4. The numbers in parentheses following each averaged value are the estimated standard deviations calculated on the assumption that the individual values are all drawn from the same population. Individual values of the Fe–N_p bond distances and their relationship to the axial ligand orientations are also shown in the figure. The two independent axial bond distances in **2** are 1.989 (4) and 2.002 (4) Å, the distances in **5** are 2.021 (6) and 2.001 (5) Å, and those in **3** are 2.018 (7) and 2.006 (7) Å. Individual

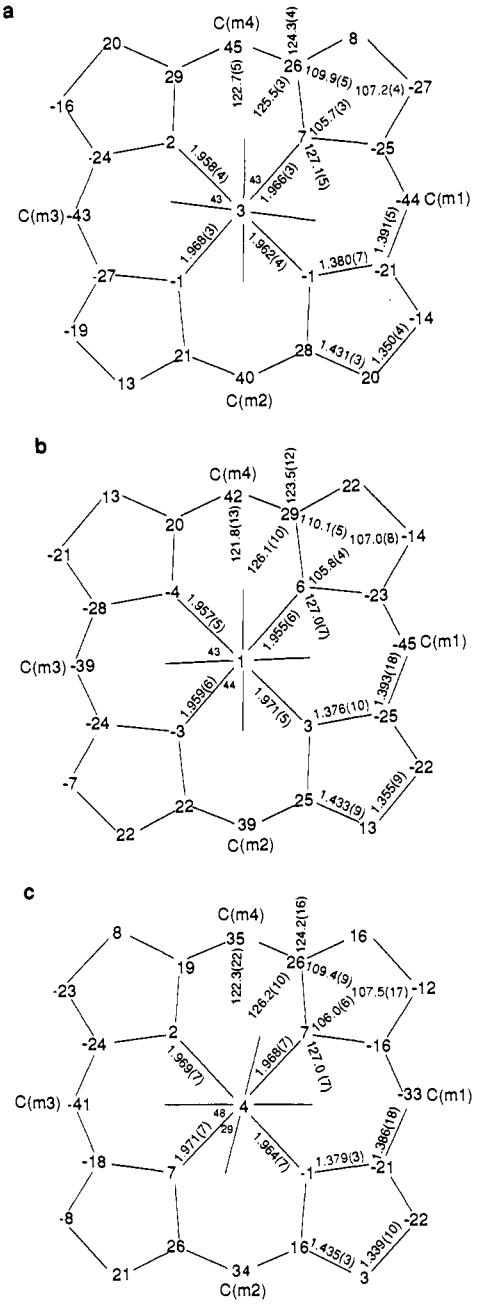

Figure 4. Formal diagram of the porphinato cores in $[Fe(TMP)(3\text{-}EtPy)_2]ClO_4$ (a), $[Fe(TMP)(4\text{-}CNPy)_2]ClO_4$ (b), and $[Fe(TMP)(3\text{-}ClPy)_2]ClO_4$ (c). Deviations of each unique atom from the mean plane of the core (in units of 0.01 Å) are shown. Averaged values for the chemically unique bond distances and angles in the core are shown. The orientation of the axial ligands with the Fe–N_p vectors and angle ϕ are shown. Individual values of the Fe–N_p bond distances are given.

bond distances and angles for the three complexes are given in the supplementary material (Tables SXV–SXX). Figure 6 also shows the displacements (in units of 0.01 Å) of the atoms from the mean plane of the respective 24-atom porphyrin core; all macrocycles are seen to be significantly S_4 ruffled. The dihedral angles between the mean core and the four mesityl groups in **2** are 87.5, 84.8, 80.1, and 86.6°; values in **5** are 83.9, 85.6, 83.5, and 84.3°; and values in **3** are 88.7, 79.2, 82.8, and 83.3°.

Due to the ruffling of the porphyrin ring, two ligand binding pockets are formed. The average perpendicular displacements of the 2,6-dimethyl groups from the mean porphyrin plane are 1.74 and 3.17 Å in **2**, 1.75 and 3.01 Å in **5**, and 1.85 and 3.03 Å in **3**. The resulting asymmetric ligand binding cavities have approximately perpendicular orientations, and as discussed previously[41] are thought to be responsible for the relative perpen-

(58) Medhi, O. K.; Silver, J. *J. Chem. Soc., Dalton Trans.* **1990**, 263–270.
(59) Epstein, L. M.; Straub, D. K.; Maricondi, C. *Inorg. Chem.* **1967**, *6*, 1720–1724.
(60) Sams, J. R.; Tsin, T. B. In *The Porphyrins*; Dolphin, D., Ed.; Academic Press: New York, 1979; Vol. IV, p 451.

Table III. Proton NMR Chemical Shifts of a Series of $[Fe(TMP)L_2]^+$ Complexes at −80 °C in CD_2Cl_2

ligand	$pK_a(BH^+)$[a]	$\delta(o\text{-}CH_3)$[b]	$\delta(p\text{-}CH_3)$[b]	$\delta(m\text{-}H)$[b]	δ(pyrr-H)[b]	δ_{iso}[c] m-H	δ_{iso}[c] pyrr-H
4-NMe_2Py	9.70	0.38	0.81	4.85	−30.9	−2.42	−39.5
2-MeHIm	7.56[d]	1.34[e]	1.44[e]	7.77[e]	−20.4[e]	+0.5[e]	−29.0[e]
N-MeIm	7.33	0.25	1.00	5.01	−31.3	−2.26	−39.9
3,4-Me_2Py	6.46	0.80	2.18	7.48	−21.1	+0.21	−29.7
3,5Me_2Py	6.15	0.67	1.79	7.12	−23.0	−0.15	−31.6
4-MePy	6.02	0.10	2.02	8.22	−18.2	+0.95	−26.8
3-MePy	5.68	1.00	2.06	8.36	−17.8	+1.09	−26.4
Py	5.22	1.27	2.40	9.47	−13.3	+2.20	−21.9
3-ClPy	2.84	1.71	2.59	10.85	−10.3	+3.58	−18.9
3-CNPy	1.45	2.30	3.21	13.07	−4.4	+5.80	−13.0
4-CNPy	1.1[f]	2.73	3.59	14.59	+2.1	+7.32	−6.5

[a] pK_a values obtained from refs 44 and 45. [b] Chemical shifts (ppm). [c] Isotropic shifts (in ppm) $\delta_{iso} = \delta_{para} - \delta_{dia}$. The diamagnetic shifts used were those of $TMPH_2$: $\delta(m\text{-}H) = 7.27$ ppm; δ(pyrr-H) = 8.62 ppm; $\delta(p\text{-}CH_3) = 2.63$ ppm; $\delta(o\text{-}CH_3) = 1.85$ ppm. [d] Corrected for the presence of $2H^+$ (0.3). [e] Average chemical shift of the multiple signals observed.[39] [f] See ref 46.

dicular orientation of the axial ligands. These cavity dimensions are similar to those observed in $[Fe(TMP)(4\text{-}NMe_2Py)_2]ClO_4$.[41]

Discussion

Pyridine ligand basicity has previously been shown to have a strong influence on the spin state of bis-ligated (porphinato)iron(III) derivatives.[52,60-65] On the basis of previous studies of (octaethylporphinato)iron(III) complexes, three important generalizations were made: Complexes with strongly basic pyridine ligands ($pK_a(BH^+) > 8.0$) are low spin,[42,60,61] and those with moderately basic pyridine ligands ($6.5 > pK_a(BH^+) > 5.0$) are also low spin,[42,57,60] but they have different structural and electronic properties than those of the strongly basic pyridine complexes. Complexes with very weakly basic pyridine ligands ($pK_a(BH^+) < 3.0$) have admixed intermediate-spin states.[52,62-65] However, all spectroscopic investigations carried out in the course of this research indicate unambiguously that *all Fe(III) complexes with TMP as porphyrin ligand are low spin*, including imidazoles and pyridines ranging in basicity from $pK_a(BH^+) = 9.70$ (4-NMe_2Py)[41,44] to 1.1[45,46] (4-CNPy), as will be discussed in detail below. The most probable reason that these low-basicity pyridines form low-spin complexes with (tetramesitylporphinato)iron(III) is because of differences in the Fe(III) d-orbital energies of $[Fe(TMP)L_2]^+$ complexes as compared to those of $[Fe(OEP)L_2]^+$ derivatives. These differences in d-orbital energies are likely caused either by differences in σ- and π-orbital energies of the porphyrin due to the peripheral substituents, or by the effects of ruffling of the porphyrin core in the TMP case (vide infra), which may lead to changes in the energies of the Fe(III) d orbitals due to the shortening of the Fe–N_p bonds.

The σ-donating properties of an axial pyridine ligand depend on the energy of the nitrogen lone pair orbital as compared to the energies of the σ-symmetry d-orbitals of iron(III). It has previously been shown[66a] that the gas-phase lone-pair ionization energies of a series of pyridines vary linearly with the basicity of the pyridine, as measured by the pK_a of its conjugate acid in aqueous solution. The energy of the σ-donating orbital of the pyridines of compounds **1–6** therefore decreases in the order 4-NH_2Py > 3-EtPy > 3-ClPy > 3-CNPy > 4-CNPy.[64,66a] The possible π interactions of pyridines with low-spin iron(III) are (i) π donation from the filled π-symmetry pyridine orbital having large electron density at the bonding nitrogen (previously called π_s[66]) to the singly occupied

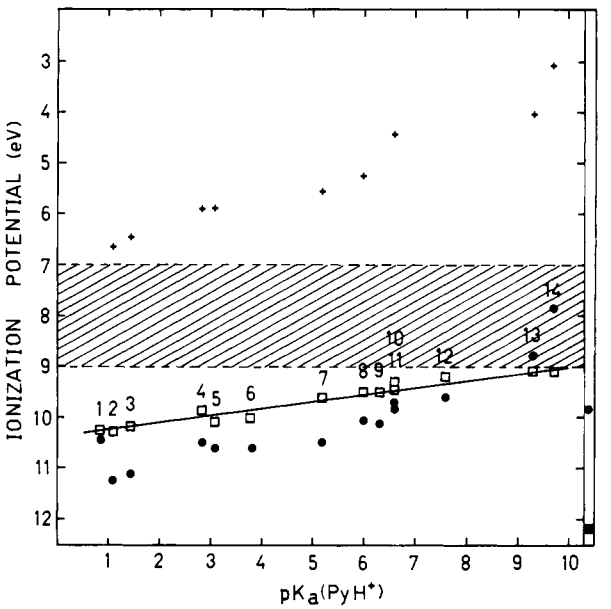

Figure 5. Plot of the ionization potentials of the n and π_s orbitals of a series of pyridines, obtained from gas-phase photoelectron spectroscopy,[66] as a function of the pK_a of their conjugate acids.[44-46] Squares: Ionization potential of the lone-pair σ-symmetry (n) orbital on the nitrogen, with correlation line reported previously.[66a] Circles: Ionization potential of the π_s orbital, which has large amplitude at the pyridine nitrogen.[66] Crosses: Relative energy of the π^* orbital of the pyridine, derived from the ionization potential of the π_s orbital[66] and the π–π^* transition energy.[67] Pyridine substituents: (1) 3,5-Cl_2; (2) 4-CN; (3) 3-CN; (4) 3-Cl; (5) 3-F; (6) 4-Cl; (7) H; (8) 4-Me; (9) 3,5-Me_2; (10) 4-OMe; (11) 3,4-Me_2; (12) 2,4,6-Me_3; (13) 4-NH_2; (14) 4-NMe_2. The energies of the lone-pair σ-symmetry (filled square) and π_2 orbital having large amplitude on the "pyridine" nitrogen (filled circle) for *N*-methylimidazole,[69] $pK_a(BH^+) = 7.33$,[61] are given for comparison in the narrow panel at the right-hand side of the diagram. The cross-hatched region between 7 and 9 eV represents the probable energies of the d orbitals of Fe(III). (The gas-phase ionization potential of the metal in iron(III) tetraphenylporphyrins is believed to lie in the 8–9-eV range,[68a] and that for iron(III) octaethylporphyrin is believed to be in the 7–8 eV range.[68b])

d_π orbital of iron or (ii) π back-donation from the filled d_π orbital of low-spin iron(III) to the empty π^* orbital of the pyridine which has a large orbital coefficient at the nitrogen (π_s). The available data showing how the energies of the σ, π_s, and π^* orbitals of pyridines depend on the pK_a of the conjugate acid of the pyridine are summarized in Figure 5.[66,67] It can be seen that the wide range of σ basicities of the pyridines of this study leads to a systematic trend in the energies of the frontier orbitals of these axial ligands. The d orbitals of iron(III) are expected to have

(61) pK_a values obtained from refs 44–46.
(62) Safo, M. K.; Scheidt, W. R.; Gupta, G. P.; Orosz, R. D.; Reed, C. A. *Inorg. Chim. Acta* **1991**, *184*, 251–258.
(63) Scheidt, W. R.; Geiger, D. K.; Hayes, R. G.; Lang, G. *J. Am. Chem. Soc.* **1983**, *105*, 2625–2632.
(64) Scheidt, W. R.; Geiger, D. K.; Haller, K. J. *J. Am. Chem. Soc.* **1982**, *104*, 495–499.
(65) Scheidt, W. R.; Geiger, D. K.; Lee, Y. J.; Reed, C. A.; Lang, G. *Inorg. Chem.* **1987**, *26*, 1039.
(66) (a) Ramsey, B. G.; Walker, F. A. *J. Am. Chem. Soc.* **1974**, *96*, 3314–3316. (b) Lichtenberger, D. L.; Walker, F. A.; Gruhn, N. E.; Bjerke, A. *J. Electron Spectrosc. Relat. Phenom.*, to be submitted for publication.
(67) Schofield, K. *Hetero-Aromatic Nitrogen Compounds, Pyrroles and Pyridines*; Plenum Press: New York, 1967.

gas-phase ionization energies in the range of 7–9 eV,[68] which positions them slightly above the energy of the lone-pair orbital of low-basicity pyridines and slightly below that of high-basicity pyridines, thus allowing a smooth variation in σ-bonding interactions throughout the series.

The σ-symmetry interactions between the metal and the axial ligands, however, are expected to be of less importance to the energies of the d_π orbitals of the complexes than are the energies of the π bonding and antibonding orbitals of the ligand donor atoms. The low energy of both π_s and π^* for 3-CNPy and 4-CNPy ensures that the main π-symmetry interaction between these ligands and low-spin iron(III) is that of π donation from the filled d_π orbital of low-spin iron(III) to the empty π^* of the pyridine (M → L π back-bonding), while the much higher energies of both π_s and π^* for the very basic pyridines, 4-NH_2Py and 4-NMe_2Py (Figure 5), suggest that the main π-symmetry interaction at this end of the basicity scale is that of π donation from the filled π_s orbital of the pyridine to the hole in the d_π orbitals of Fe(III) (L → M π donation). Thus, 3-CNPy and 4-CNPy are expected to be relatively strong π acceptors while 4-NMe_2Py and 4-NH_2Py are expected to be relatively strong π donors. Somewhere in the middle of this $pK_a(BH^+)$ range, pyridine ligands may be neither π acceptors nor π donors to iron(III) (or weakly both). For comparison, the ionization energies of the σ and π_s orbitals of *N*-methylimidazole,[69] which has been said to act as a π donor to low-spin Fe(III) hemes,[36,42] are marked on the right-hand side of the diagram with solid squares and circles, respectively.

Structures of the Complexes. The structures of the three complexes reported herein have perpendicular axial ligand plane orientations, as does **6**, whose preliminary structure is very similar to those of the other three. An ORTEP plot of **2**, a representative structure, is shown in Figure 3. As for almost all other (porphinato)iron(III) complexes with relative perpendicular axial ligand orientations, complexes **2**, **3**, and **5** have strongly S_4 ruffled porphinato cores. We have previously suggested[41] that the ruffled core and the relative perpendicular axial ligand orientation are closely related phenomena that represent the most favorable solution to the steric problems involved in the formation of low-spin bis-ligated complexes of iron(III) porphyrinates with hindered imidazoles or pyridines. Briefly, for low-spin pyridine-ligated complexes, the steric requirements are such that the projection of the pyridine plane onto the porphyrin plane requires an angle of ~45° from an Fe–N_p vector to avoid unfavorable steric interaction between the pyridine α-hydrogen atoms and the porphyrin nitrogen atoms. To avoid sterically unfavorable contacts between the mesityl methyl groups and the pyridine ligand requires tipping the mesityl rings away from the axial ligand, which results in an S_4 ruffled core and orthogonal ligand binding pockets on the two sides of the porphyrin. Finally, another important consequence of the strongly ruffled porphinato core is that it leads to a substantial foreshortening of the Fe–N_p bonds, as observed for complexes **2**, **3**, and **5**; it is a reasonable presumption that these shortened Fe–N_p bonds lead to both stronger σ and π interactions between the porphyrin and the iron(III) center.

EPR Spectra of the Complexes. As described in the Results section, complexes **2**–**6** exhibit unique EPR spectra among low-spin iron(III) porphyrinates, whereas **1** has a "normal" "large g_{max}" type of EPR spectrum with a g value of 3.40 (Table II). Complexes **2** and **3**, with perpendicularly aligned axial ligands (Figure 3), have single-feature "large g_{max}" type EPR spectra, having the "ramp-type" shape previously associated with this type of signal,[70] but with unusually low g values of 2.9–3.2, as listed in Table II. These are the first low-spin iron(III) porphyrins for which such low g value single-feature EPR spectra have been observed. This result clearly shows that perpendicular axial ligand orientation is not necessarily associated with $g \geq 3.4$. Even though the crystal structure of complex **4** has not yet been determined, we believe that the 2-MeHIm ligands are held in perpendicular planes. This belief is based on the EPR spectrum of the complex, which reveals the same single-feature "large g_{max}" type of EPR spectrum as **2** and **3**, but also with an unusually low g value. The assumption made for **4** is also consistent with Mössbauer quadrupole splittings discussed below, the structures of related complexes,[41,71] and recent 2-D NMR investigations of $[Fe(TMP)(2\text{-MeHIm})_2]ClO_4$ at low temperatures in CD_2Cl_2 solution.[38] $[Fe(TMP)(4\text{-CNPy})_2]ClO_4$, **5**, and $[Fe(TMP)(3\text{-CNPy})_2]ClO_4$, **6**, have also unusual EPR spectra, which are *axial*, with $g_\perp = 2.53$ and $g_\parallel = 1.56$ or $g_\perp = 2.62$ and $g_\parallel$ unresolved. These axial EPR spectra indicate a change in the electronic ground state of low-spin Fe(III),[48–50] as is discussed below.

The Griffith theoretical treatment for the EPR spectra of low-spin Fe(III) describes the wave function of the unpaired electron as being composed of some fraction of each of the three non-σ-bonding d-orbitals.[48–50,72] The mixing coefficients, a, b, and c, for the three d-orbitals of interest, d_{xz}, d_{yz}, and d_{xy}, respectively, have been calculated from the EPR g values of the complexes having extremes in pyridine basicity: For $[Fe(TMP)(4\text{-NMe}_2\text{Py})_2]ClO_4$, with $g_z = 3.44$, $g_y = 1.80$, and $g_x = 0.92$,[41] $a = 0.89$, $b = 0.43$, and $c = 0.15$ (~79% d_{xz}, 19% d_{yz}, 2% d_{xy}), while for $[Fe(TMP)(4\text{-CNPy})_2]ClO_4$, in the "proper axis system" of Taylor,[48] which defines the z axis as being perpendicular to the plane of the heme ($g_z = -1.56$, $g_y = 2.53$, $g_x = -2.53$), $a = 0.18$, $b = 0.18$, and $c = 0.96$, indicating a shift in electronic ground state to a predominantly d_{xy} unpaired electron configuration (~93% d_{xy}, 3% d_{yz}, 3% d_{xz}).

Mössbauer Spectra of the Complexes. Mössbauer quadrupole splittings can also be used to gain information concerning the relative orientations of axial ligand planes. We have previously noted,[41] as has Silver,[73] that ΔE_Q values of ≥ 2.1 mm/s suggest relative parallel axial ligand orientations, while ΔE_Q values of less than 2.0 mm/s suggest relative perpendicular alignment of the axial ligand planes. For the complexes of this study, however, the quadrupole splittings are extremely small. For the same complexes, **2**, **3**, **4**, and **5**, which have unusually low single-feature g values, unusually small quadrupole splittings $1.4 > \Delta E_Q > 0.97$ mm/s are also observed. The ΔE_Q values for all $Fe^{III}(TMP)$ complexes investigated thus far are listed in Table II.

The magnitude of the quadrupole splitting in low-spin hemins is related to the electronic asymmetry about the ^{57}Fe nucleus. The electric field gradient (QV_{zz} and asymmetry parameter η are given by[74]

$$QV_{zz}/4 = (a^2/2 + b^2/2 - c^2)(1.5 \text{ mm/s}) \quad (1)$$

$$\eta = (V_{xx} - V_{yy})/V_{zz} = -(3/2)(a^2 - b^2)/(a^2/2 + b^2/2 - c^2) \quad (2)$$

where a, b, and c are the orbital coefficients defined above. If the single electron were equally distributed among the three orbitals ($a^2 = b^2 = c^2 = 0.33$) then eq 1 would predict that the electric field gradient would be zero, as would the asymmetry parameter, as well as the quadrupole splitting:[75]

$$\Delta E_Q = (QV_{zz}/2)(1 + \eta^2/3)^{1/2} \quad (3)$$

In the case of $Fe(CN)_6^{3-}$, the quadrupole splitting is ~0.46 mm/s at 77 K, and strongly temperature dependent (0.53 mm/s at 20 K to 0.28 mm/s at 300 K).[75] The 77 K value is considerably smaller than any of the quadrupole splittings measured in the low-spin iron(III) porphyrinates of this study (Table II). As the orbital of the unpaired electron gains more than $^1/_3$ d_{xy} character, the electric field gradient, V_{zz}, should become increasingly negative (eq 1); the asymmetry parameter will remain zero if the coeffi-

(68) (a) Khandelwal, S. C.; Roebber, J. L. *Chem. Phys. Lett.* **1975**, *34*, 355. (b) Kitagawa, S.; Morishima, I.; Yonezawa, T.; Sato, N. *Inorg. Chem.* **1979**, *18*, 1345. (c) Lichtenberger, D. L.; Walker, F. A.; Nebesny, K. W.; Ray, C. D., unpublished data.
(69) Ramsey, B. G. *J. Org. Chem.* **1979**, *44*, 2093.
(70) Salerno, J. C. *J. Biol. Chem.* **1984**, *259*, 2331–2336.
(71) Scheidt, W. R.; Kirner, J. L.; Hoard, J. L.; Reed, C. A. *J. Am. Chem. Soc.* **1987**, *109*, 1963–1968.
(72) Griffith, J. S. *Proc. R. Soc. London, A* **1956**, *235*, 23–36.
(73) Medhi, O. K.; Silver, J. *J. Chem. Soc., Dalton Trans.* **1990**, 555–559.
(74) Lang, G.; Marshall, W. *Proc. Phys. Soc.* **1966**, *87*, 3–34.
(75) Oosterhuis, W. T.; Lang, G. *Phys. Rev.* **1969**, *178*, 439–456.

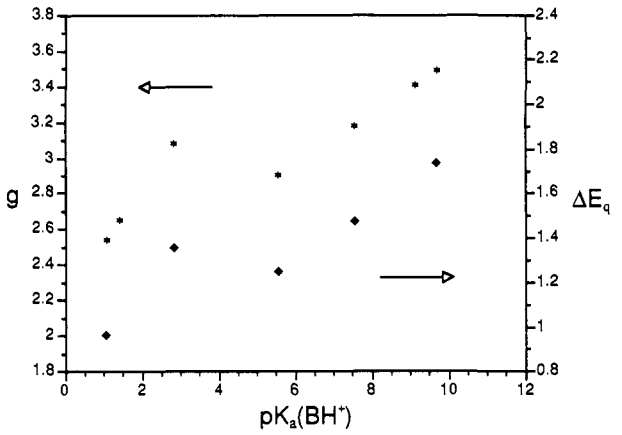

Figure 6. Plot of ΔE_Q and g value of the $[Fe(TMP)L_2]ClO_4$ complexes versus the pK_a of the conjugate acid of the ligand.

cients a and b are equal, as they are in the case of axial EPR signals such as those of the $(3\text{-CNPy})_2$ and $(4\text{-CNPy})_2$ complexes. For the orbital coefficients given above for the 4-CNPy complex, eqs 1–3 give $\Delta E_Q = -2.67$ mm/s, which is considerably larger than that observed (0.97 mm/s) or that observed for even the most basic pyridine complex of $Fe(TMP)OClO_3$, that of 4-NMe_2Py (1.74 mm/s observed; +2.11 mm/s calculated from eqs 1–3). However, the scaling factor of 1.5 mm/s in eq 1 is based on the observation that a single d electron usually gives a quadrupole splitting of about 3 mm/s.[74] It should be noted, however, that this value of the scaling factor does not take into consideration the effect of ligand charges and covalency of their interaction with the metal; most values of the quadrupole splitting constant ΔE_Q for low-spin Fe(III) hemes are, in fact, lower than 3 mm/s.[29,41,73-79] In addition, eqs 1–3 do not take into account lattice contributions to ΔE_Q. From the above analysis of the data presented in this paper, it now appears that the observed Mössbauer and EPR parameters of the siroheme center of *D. vulgaris* sulfite reductase[76] and the heme d of the *Thiobacillus denitrificans* nitrate reductase[77] suggest an electronic ground state which is $(d_{xz},d_{yz})^4(d_{xy})^1$ in the proper axis system (z perpendicular to the heme plane) ($\Delta E_Q = -2.52$ mm/s[76,80] and -1.70 mm/s,[77,80] respectively, with η small and positive in each case, and $g_y = 2.44$, $g_x = -2.36$, $g_z = -1.77$,[76,80] and $g_y = 2.50$, $g_x = -2.43$, $g_z = -1.70$,[77,80] respectively).

The breadth of the Mössbauer spectra of the low-basicity pyridine complexes of $Fe(TMP)OClO_4$ at 4.2 K in both zero and applied field, mentioned in the Results section above, is also related to the orbital of the unpaired electron having considerable d_{xy} character. As suggested previously by Lang,[78,79] in this case H_{eff} is approximately proportional to cos Θ, where Θ is the angle between H_{eff} and the plane of the orbital of the unpaired electron. The result is an almost uniform distribution of H_{eff} values between zero and the maximum, yielding a spectrum without well-defined lines. Interestingly, the Mössbauer spectrum of the siroheme iron of *D. vulgaris* sulfite reductase, derived from subtraction of the sharper signal of the Fe_4S_4 signal, is broad at 4.2 K.[76]

In line with the above-discussed relationship between EPR and Mössbauer data, a correlation can be made between either the g values or the ΔE_Q values and the axial ligand basicity. As can be seen from Figure 6, the value of the quadrupole splitting decreases with decreasing pK_a of the conjugate acid of the pyridine ligand. (The value of ΔE_Q for the complex in which the ligands are 2-MeHIm, **4**, also falls on this correlation line, as is shown in Figure 6.) Such a correlation of ΔE_Q with the basicity of the ligand has not previously been reported for low-spin iron(III) porphyrinates.[81] The EPR maximum g values also vary linearly with the basicity of the axial pyridine ligands (Figure 6). This correlation shows the reverse $pK_a(BH^+)$ relationship to that reported previously for a series of bis-pyrazole and bis-indazole complexes of $TPPFe^{III}$.[42] The reason for the deviations of the 3-chloropyridine complex from the linear correlation may be related to the relatively large deviations of the $[Fe(TMP)(3\text{-ClPy})_2]ClO_4$ structure from an ideal D_{2d} geometry. Not surprisingly, the Mössbauer quadrupole splittings and EPR g values are strongly correlated with each other (not shown).

The unusually small ΔE_Q and g values for the low-basicity pyridine systems may be explained by considering the ligand π-bonding properties, as suggested by the trends in the π_s and π^* orbital energies presented in Figure 5. In terms of a simple molecular orbital theory treatment of the π-bonding effects of the axial ligands, if the energies of the d_π orbitals of the metal are similar to those of the filled π orbital of the axial ligand having large amplitude on the donor atom (π_s), then the energy of the resulting π-symmetry molecular orbitals having greatest metal character will be at higher energy than they would have been in the absence of the interaction with the filled π orbitals of the ligand. This condition thus ensures that the MO equivalents of d_{xz} and d_{yz} will be at higher energy than d_{xy} and that the ground state will be $(d_{xy})^2(d_{xz},d_{yz})^3$, as observed for bis-imidazole and the high-basicity pyridine complexes studied, 4-NH_2Py and 4-NMe_2Py.[41] On the other hand, if the energies of the d_π orbitals of the metal are similar to those of the empty π orbital of the axial ligand having large amplitude on the donor atom, then the energy of the resulting π-symmetry molecular orbitals having greatest metal character will be at lower energy than they would have been in the absence of the interaction with the empty π orbitals of the ligand, thus lowering the energies of the MO equivalents of d_{xz} and d_{yz} from those expected in the absence of the interaction with the empty π orbitals on the ligand. This stabilization of d_{xz} and d_{yz} can lead, in the limit, to their being lower in energy than d_{xy}, and thus the $(d_{xz},d_{yz})^4(d_{xy})^1$ electronic ground state results, as observed for the $(3\text{-CNPy})_2$ and $(4\text{-CNPy})_2$ complexes of Fe^{III}-(TMP).

NMR Spectra of the Complexes. Since NMR spectroscopy is expected to be the most sensitive tool for detecting variation in electron spin density, an investigation of the ^1H NMR spectra of a series of low-spin Fe(III) complexes of the type $[Fe(TMP)(L)_2]^+$ was undertaken at −80 °C, where ligand exchange does not contribute to the observed chemical shifts of even the least basic pyridine complexes. Likewise, ligand rotation is expected to be slow below −60 °C for all pyridine complexes, based upon studies of the temperature dependence of the α- and α'-H of 3-picoline bound to $Fe^{III}(TMP)$.[38] The ^1H chemical shifts of these complexes are summarized in Table III, where it is clearly shown that the chemical shifts of all TMP and pyridine ligand protons vary with the basicity of the pyridine ligand. The most dramatic variation is that observed for the pyrrole-H of the series of complexes, for which the observed chemical shift at −80 °C varies from the very strongly upfield-shifted position of 4-NMe_2Py (~31 ppm) typical of bis-imidazole complexes to well into the diamagnetic region (~2 ppm) for 4-CNPy. This trend appears to parallel those observed for EPR g values and Mössbauer quadrupole splitting constants (Figure 6). The linearity of this trend is confirmed in Figure 7, indicating a smooth transition into an electron configuration that is largely the previously-observed[18-22,30-38] $(d_{xy})^2(d_{xz},d_{yz})^3$ to one that has significant $(d_{xz},d_{yz})^4(d_{xy})^1$ character, as discussed below.

Some time ago La Mar and co-workers[83] showed that similar pyrrole-H resonance shifts are observed for a series of $[Fe(TPP)(L)_2]^+$ complexes with para-substituted pyridines and that

(76) Huynh, B. H.; Kang, L.; DerVartanian, D. V.; Peck, H. D.; LeGall, J. *J. Biol. Chem.* **1984**, *259*, 15373–15376.
(77) Huynh, B. H.; Lui, M. C.; Moura, J. J. G.; Moura, I.; Ljungdahl, P. O.; Munck, E.; Payne, W. J.; Peck, H. D.; DerVartanian, D. V.; LeGall, J. *J. Biol. Chem.* **1982**, *257*, 9576–9581.
(78) Lang, G. *Q. Rev. Biophys.* **1970**, *3*, 1–60.
(79) Lang, G.; Oosterhuis, W. T. *J. Chem. Phys.* **1969**, *51*, 3608–3614.
(80) Huynh, B. H., personal communication.
(81) This observation is true only for porphyrinate derivatives. For example, Johnson and Shepherd[82] have reported a decrease in the Mössbauer quadrupole splitting as the ligand pK_a decreases for a series of pyridine complexes of $[(CN)_5FeL]^{2-}$.
(82) Johnson, C. R.; Shepherd, R. E. *Inorg. Chem.* **1983**, *22*, 3506.
(83) La Mar, G. N.; Bold, T. J.; Satterlee, J. D. *Biochim. Biophys. Acta* **1977**, *498*, 189.

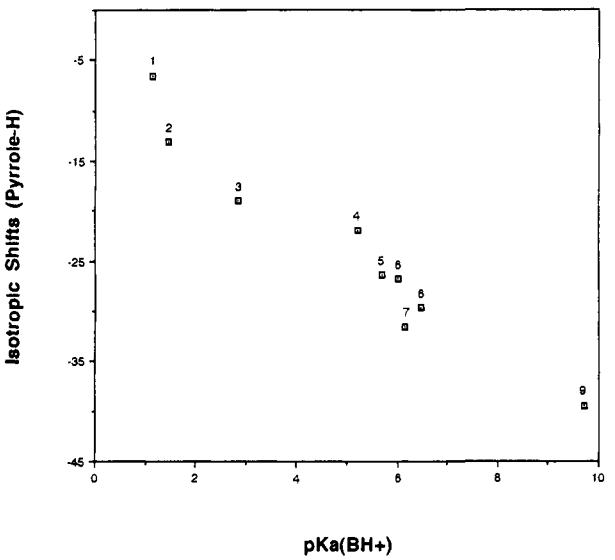

Figure 7. Plot of the pyrrole-H isotropic shift for a series of $[Fe(TMP)L_2]^+$ complexes in CD_2Cl_2 at −80 °C versus the pK_a of the conjugate acid of the ligand. Pyridine substituents: (1) 4-CN; (2) 3-CN; (3) 3-Cl; (4) H; (5) 3-Me; (6) 4-Me; (7) 3,5-Me_2; (8) 3,4-Me_2; (9) 4-NMe_2. The pyrrole-H hyperfine shift of the $(N\text{-MeIm})_2$ complex (−39.9 ppm) is very similar to that of the $(4\text{-NMe}_2\text{Py})_2$ complex, and the average pyrrole-H hyperfine shift of the $(2\text{-MeHIm})_2$ complex (−29.0 ppm) is between that of the $(4\text{-MePy})_2$ and $(3,4\text{-Me}_2\text{Py})_2$ complexes, even though the pK_as of the conjugate acids of these two ligands are 7.33 and 7.56, respectively.[61] Thus, by NMR isotropic shift criteria, imidazoles appear to be relatively better π donors than pyridines of the same σ basicity.

the pyrrole-H resonance of the TPP shifts downfield as the basicity of the pyridine decreases.[84] The isotropic shifts of the pyrrole-H protons of the TPP complexes reported previously, in $CDCl_3$ at −60 °C, range from −37.9 ppm (L = 4-NMe_2Py) to −15.9 ppm (L = 4-CNPy), corresponding to a total shift difference of 22 ppm.[83] In the present case of the $TMPFe^{III}$ complexes, the trend is considerably more pronounced; the pyrrole-H shifts span a range of about 33 ppm at −80 °C, yet all are low-spin Fe(III) complexes. The larger range in pyrrole-H shifts of the TMP complexes of the present study and the TPP complexes of the same axial ligands reported previously[83] does not result from an intrinsic difference in the porphyrin orbital energies of the low-spin Fe(III) complexes of these two porphyrins, since the $(N\text{-MeIm})_2$ complexes of the two have very similar g values (2.89, 2.33, 1.75 (TMP);[41] 2.89, 2.29, 1.55 (TPP)[42]). Rather, the larger range results from the requirement that all pyridine complexes of Fe^{III}(TMP) have ligands in perpendicular planes, while at least the 4-NMe_2Py complex of Fe^{III}(TPP) has the axial ligands in parallel planes, based on the EPR spectral type[42] and the similarity to $[Fe(OEP)(4\text{-NMe}_2\text{Py})_2]ClO_4$.[41]

The difference in the pyrrole-H shifts for L = 4-NMe_2Py and 4-CNPy is partly due to differences in the dipolar contribution to the isotropic shift, as suggested previously.[83] By using the appropriate geometric factors[83] and g anisotropies to calculate the dipolar contributions to the isotropic shifts, it can be shown that −30.6 ppm of the isotropic shift of the pyrrole-H of $[Fe(TMP)(4\text{-NMe}_2\text{Py})_2]^+$ and −15.2 ppm of that of $[Fe(TMP)(4\text{-CNPy})_2]^+$ are due to the contact contribution.[87] This smaller contact contribution to the isotropic shift of the 4-CNPy complex is consistent with the electron configuration having considerable $(d_{xz},d_{yz})^4(d_{xy})^1$ character.

Simonneaux and co-workers[88] recently reported a thorough study of the ^1H NMR spectrum of the bis(*tert*-butyl isocyanide) (*t*-BuNC) complex of $[Fe(TPP)OClO_3]$. They found that the pyrrole-H, as well as all other resonances of the TPP ligand, resonated in the diamagnetic region of the spectrum, yet showed Curie behavior, with the pyrrole-H resonance shifting to lower shielding as the temperature is lowered. They concluded that the pattern of shifts observed was indicative of the unpaired electron being localized in the d_{xy} orbital of low-spin Fe(III).[88] In agreement with this conclusion, the EPR spectrum of $[Fe(TPP)(t\text{-BuNC})_2]ClO_4$ is axial ($g_\parallel = 1.906$, $g_\perp = 2.192$),[89] and the calculated coefficients ($a = 0.064$, $b = 0.064$, $c = 0.985$) indicate that the ground-state orbital of the unpaired electron is 97% d_{xy}. The dipolar contributions to the isotropic shifts are small because of the much smaller g anisotropy ($g_\parallel^2 - g_\perp^2 = 1.17$), yielding a predicted dipolar shift of the pyrrole-H of +2.5 ppm and a derived contact shift of ~+0.5 ppm at −80 °C. This is consistent with the fact that the d_{xy} orbital cannot be involved in π spin delocalization to or from the metal and, because of nodes at the porphyrin nitrogens, is expected to yield negligible σ spin delocalization.[36] Thus, the estimated contact shifts for the pyrrole-H of $[Fe(TMP)(4\text{-NMe}_2\text{Py})_2]^+$ and $[Fe(TMP)(4\text{-CNPy})_2]^+$ mentioned above suggest that if the orbital of the unpaired electron of the former is mainly d_{xz},d_{yz} in nature then that of the latter is composed of approximately half of the electronic state that is mainly d_{xy} in nature and half of that which is mainly d_{xz},d_{yz} in nature *at −80 °C*. In support of this conclusion is the fact that the temperature dependence of $[Fe(TMP)(3\text{-CNPy})_2]^+$ exhibits anti-Curie behavior, with the pyrrole-H peak shifting *upfield* (away from its diamagnetic position) as the temperature is raised.[87] This suggests that, for the Fe^{III}(TMP) complex of 3-CNPy, the mainly $(d_{xz},d_{yz})^4(d_{xy})^1$ electron configuration is the ground state, but the mainly $(d_{xy})^2(d_{xz},d_{yz})^3$ state is thermally accessible to an increasing extent over the temperature range of the NMR investigations (−90 to +20 °C). A detailed investigation of the temperature dependence of these and other tetrakis(2,6-disubstituted phenyl)porphyrin complexes of Fe(III) is in progress and will be reported elsewhere.[87] It should be noted, however, that the large temperature difference between the EPR and NMR measurements (77 K vs 193 K), together with the thermal population of the mainly $(d_{xy})^2(d_{xz},d_{yz})^3$ excited state of the complexes having weakly basic ligands, as well as the ~7% (d_{xz},d_{yz}) character of the ground-state orbital of the unpaired electron, can easily account for the observed contact contribution to the isotropic shift of the 3- and 4-CNPy complexes at −80 °C. Thus, in spite of the large difference in temperature between the NMR (193 K) and the EPR and Mössbauer (77 K and below) spectral measurements, the NMR data in all respects support the conclusions reached on the basis of low-temperature EPR and Mössbauer data, and in addition indicate the high efficiency of M → L π back-donation as a means for spin delocalization in low-spin iron(III) porphyrins having ground states which are largely d_{xy} in nature. Further exploration of such systems is in progress.

A recent ^1H NMR study of the extremely sterically hindered bis(2-methylbenzimidazole) complex of Fe(TMP)Cl showed that the four closely-spaced pyrrole-H resonances have chemical shifts of ~+1 ppm at −58 °C, with anti-Curie temperature dependence.[90] The magnetic moment of the complex at 200 K indicates that it is low spin, and the single-feature EPR spectrum has g = 2.6.[90] Thus, it appears that this complex, $[Fe(TMP)(2\text{-MeHBzim})_2]^+$, has a similar amount of $(d_{xz},d_{yz})^4(d_{xy})^1$ character to its ground state as does that of $[Fe(TMP)(4\text{-CNPy})_2]^+$, and considerably more than $[Fe(TMP)(2\text{-MeHIm})_2]^+$ (Tables II and III). Although the structures of neither of these hindered imidazole complexes have been determined in the solid state, it is logical to expect the porphyrin ring of the 2-methylbenzimidazole complex to be more ruffled than that of the 2-methylimidazole complex. It therefore appears that the extent of ruffling of the porphyrin

(84) Hill and Morallee[85] previously reported a similar trend for a series of $[Fe(Proto\ IX)L_2]^+$, where L is a series of pyridines (heme methyl peaks shift downfield as the basicity of the pyridine decreases).

(85) Hill, H. A. O.; Morallee, K. G. *J. Am. Chem. Soc.* **1972**, *94*, 731–738.

(86) Jesson, J. P. In *NMR in Paramagnetic Molecules*; La Mar, G. N., Horrocks, W. D., Holm, R. H., Eds.; Academic Press: New York, 1973; Chapter 1.

(87) Watson, C. T.; Simonis, U.; Walker, F. A., manuscript in preparation.

(88) Simonneaux, G.; Hindre, F.; LePlouzennec, M. *Inorg. Chem.* **1989**, *28*, 823.

(89) Safo, M. K.; Scheidt, W. R., unpublished data.

(90) Nakamura, M.; Nakamura, N. *Chem. Lett. (Jpn.)* **1991**, 1885.

ring, in addition to axial ligand π donor/acceptor effects, may influence the choice of electronic ground state in low-spin iron(III) porphyrins. Further investigations of the possible role(s) of porphyrin ring ruffling are in progress in our laboratories.

Summary. On the basis of EPR, Mössbauer, and ^{1}H NMR investigations, the present study suggests that as the π and π^* orbital energies of the pyridine ligands vary either the $(d_{xy})^2(d_{xz},d_{yz})^3$ or the $(d_{xz},d_{yz})^4(d_{xy})^1$ ground state can be stabilized within a group of isostructural complexes. The $(d_{xy})^2(d_{xz},d_{yz})^3$ ground state is stabilized when the filled π_s orbital of the pyridine is similar to the energy of the d-orbitals of Fe(III) (high-basicity pyridines), while the $(d_{xz},d_{yz})^4(d_{xy})^1$ ground state is stabilized when the empty π^* orbital of the pyridine is similar to the energy of the d-orbitals of iron(III) (low-basicity pyridines). The EPR spectra at 77 K and below reveal unusual, not previously observed, features for pyridines of intermediate or low basicity, with the EPR spectra having either a single feature of lower g value than those previously called "large g_{max}" signals ($g > 3.4$) or axial, with $g_\parallel < g_\perp$. For the same complexes unusually low Mössbauer quadrupole splittings ($1.4 > \Delta E_Q > 0.97$ mm/s) are observed at 77 K. EPR g values and Mössbauer ΔE_Q values can be linearly correlated with the basicity of the axial ligands, although the probable reason for these linear correlations is the smooth change in the balance of π_s vs π^* interactions of the axial ligands with the d-orbitals of Fe(III). The linear relationship is also valid for the correlation of the NMR isotropic shifts of the pyrrole protons with the pK_a of the conjugate acid of the pyridine ligands. At the much higher temperature of the NMR measurements, 193 K, the orbital of the unpaired electron appears to change smoothly from mainly $(d_{xy})^2(d_{xz},d_{xy})^3$ (high-basicity pyridines) to an equilibrium mixture that contains at least 50% $(d_{xz},d_{yz})^4(d_{xy})^1$ (low-basicity pyridines). This equilibrium mixture is temeprature dependent, leading to anti-Curie temperature dependence of the isotropic shifts of low-basicity pyridine complexes. The large contact contribution to the *meso*-phenyl *m*-H isotropic shifts of the latter complexes is consistent with the ground state being the mainly $(d_{xz},d_{yz})^4(d_{xy})^1$ configuration, in which π spin delocalization occurs from the *nominally filled* (93% filled) d_{xz},d_{yz} orbitals of the metal to the empty $4e(\pi)$ orbitals of the porphyrin ($M \rightarrow L$ π back-bonding). The unusual spectroscopic properties predict the perpendicular orientation of the axial ligands, at least when these axial ligands are pyridines. This result is supported by the crystal structures of three of the present complexes, which establish the perpendicular alignment and further show extreme S_4 ruffling of the porphinato core. It is interesting to note that the structural parameters ($Fe-N_{ax}$ and $Fe-N_P$ bond lengths, degree of core ruffling, etc.) are effectively constant for the three complexes of this study and $[Fe(TMP)(4\text{-}NMe_2Py)_2]ClO_4$,[42] despite the systematic changes in spectroscopic properties.

Relevance of the Results of This Work to the Interpretation of the Spectroscopic Properties of Reduced ("Green") Heme-Containing Systems. The results presented in this paper are significant in providing not only greater understanding of the possible electronic ground states of low-spin iron(III) porphyrinates and the complementary information provided by EPR, Mössbauer, and NMR spectroscopic data but also to a more complete understanding of the spectroscopic properties of the so-called "green hemes"—iron chlorins, bacteriochlorins, and isobacteriochlorins that are found in various biological systems. The EPR spectra of low-spin "green hemes" are all near-axial ($[Fe(OEC)(N\text{-}MeIm)_2]^+$: $g_1 = 2.51$, $g_2 = 2.37$, $g_3 = 1.73$;[91] $[Fe(OEiBC)(N\text{-}MeIm)_2]^+$: $g_1 = 2.49$, $g_2 = 2.37$, $g_3 = 1.71$;[91] heme d_1 of *Pseudomonas* cytochrome oxidase: $g_1 = 2.52$, $g_2 = 2.42$, $g_3 = 1.73$;[49] the seroheme center of *D. vulgaris* sulfite reductase: $g_1 = 2.44$, $g_2 = 2.36$, $g_3 = 1.77$;[76] and the heme d of *Thiobacillus denitrificans* nitrite reductase: $g_1 = 2.50$, $g_2 = 2.43$, $g_3 = 1.70$[77]). The orbital of the unpaired electron in several cases has previously been assigned as mainly d_{xy}.[48-50] In these cases, it is probable that the d_{xy} orbital is higher in energy than d_{xz} and d_{yz} because of the significantly stronger σ-donor properties of the reduced hemes as compared to their porphyrin counterparts; in terms of crystal field theory, these stronger σ-donor properties are expected to destabilize $d_{x^2-y^2}$ relative to d_{z^2}, and at the same time destabilize d_{xy} relative to d_{xz},d_{yz}. On the basis of the results of the present study, it is possible that the Mössbauer quadrupole splitting, ΔE_Q, and the electric field gradient, V_{zz}, are both intrinsically negative, while η is small and positive, in these "green heme"-containing systems.

Acknowledgment. We thank the National Institutes of Health for support of this research under Grants GM-38401 (W.R.S.), DK-31038 (F.A.W.), and HL-16860 to George Lang (G.P.G.). We also acknowledge helpful discussions with Professor B. H. Huynh.

Supplementary Material Available; Complete crystal data and intensity collection parameters (Table SI), final atomic coordinates for $[Fe(TMP)(3\text{-}EtPy)_2]ClO_4$, $[Fe(TMP)(4\text{-}CNPy)_2]ClO_4$, and $[Fe(TMP)(3\text{-}ClPy)_2]ClO_4$ (Tables SII–SIV), anisotropic thermal parameters and fixed hydrogen atom positions for $[Fe(TMP)(3\text{-}EtPy)_2]ClO_4$ and $[Fe(TMP)(4\text{-}CNPy)_2]ClO_4$ (Tables SV, SVI, SVIII, and SIX), anisotropic thermal parameters, fixed hydrogen atom positions, and fixed perchlorate atom coordinates and group parameters for $[Fe(TMP)(3\text{-}ClPy)_2]ClO_4$ (Tables SXI–SXIII), bond distances and bond angles for $[Fe(TMP)(3\text{-}EtPy)_2]ClO_4$ (Tables SXV and SXVI), bond distances and bond angles for $[Fe(TMP)(4\text{-}CNPy)_2]ClO_4$ (Tables SXVII and SXVIII), and bond distances and bond angles for $[Fe(TMP)(3\text{-}ClPy)_2]ClO_4$ (Tables SXIX and SXX) (49 pages); listing of structure factors for $[Fe(TMP)(3\text{-}EtPy)_2]ClO_4$, $[Fe(TMP)(4\text{-}CNPy)_2]ClO_4$, and $[Fe(TMP)(3\text{-}ClPy)_2]ClO_4$ (Tables SVII, SX, and SXIV) (79 pages). Ordering information is given on any current masthead page.

(91) Stolzenberg, A. M.; Strauss, S. H.; Holm, R. H. *J. Am. Chem. Soc.* **1981**, *103*, 4763–4778.